Journal of King Saud University – Science 34 (2022) 102059

Contents lists available at ScienceDirect

Journal of King Saud University – Science

journal homepage: www.sciencedirect.com

Original article

Ananas comosus waste mediated highly stable Au NPs for environmental and biological applications

Maninder Singh [a], Ravneet Kaur [b], Jagpreet Singh [c,d,*], Mohit Rawat [a,*,#], Harpreet Kaur [b], Sanjeev Kumar [b,*], Tahani Awad Alahmadi [e], Sulaiman Ali Alharbi [f], Milton Wainwright [g], Abdullah Mohamed [h]

[a] *Department of Nanotechnology, Sri Guru Granth Sahib World University, Fatehgarh Sahib 140406, Punjab, India*
[b] *Department of Physics, Sri Guru Granth Sahib World University, Fatehgarh Sahib 140406, Punjab, India*
[c] *Department of Chemical Engineering, Chandigarh University, Gharuan, Mohali 140413, India*
[d] *University Centre for Research and Development, Chandigarh University, Gharuan, Mohali 140413, India*
[e] *Department of Pediatrics, College of Medicine and King Khalid University Hospital, King Saud University, Medical City, PO Box 2925, Riyadh 11461, Saudi Arabia*
[f] *Department of Botany and Microbiology, College of Science, King Saud University, PO Box 2455, Riyadh 11451, Saudi Arabia*
[g] *Department of Molecular Biology and Biotechnology, University of Sheffield, Sheffield S10 2TN, United Kingdom*
[h] *Research Centre, Future University in Egypt, New Cairo 11745, Egypt*

ARTICLE INFO

Article history:
Received 28 January 2022
Revised 10 April 2022
Accepted 23 April 2022
Available online 29 April 2022

Keywords:
Au NPs
Green synthesis
Catalysis
Antimicrobial
Photocatalysis

ABSTRACT

In contemporary times, the development of a cost-effective and sustainable platform for mitigating water pollutants is an ongoing challenge. Herein, *Ananas comosus* waste leaves mediated Au NPs have been synthesized after optimization of various reaction parameters and are found highly stable (for one year). The formation of Au NPs is confirmed by various characterization techniques i.e., UV–Visible spectrophotometer, FTIR, SAED, and HRTEM. UV–Vis spectrum displays the surface plasmon wavelength around 520 nm. HRTEM images show that the synthesized Au NPs are in narrow size distribution having size range between 20 and 30 nm with different shapes. Furthermore, they are employed as the effective catalyst, photocatalyst, and antimicrobial agents for the conversion reduction of 4-nitrophenol (20 min), methylene blue dye degradation (90 min), and *Escherichia coli* (inhibition zone 16 mm), and *Bacillus subtilis* (inhibition zone 13 mm) bacteria, respectively. Thus, this study offers a positive step in material research to prepare efficient photocatalyst, catalysts, and antimicrobial agents via a cost-effective and sustainable approach.

1. Introduction

Water is a fundamental component of everyday life that preserves numerous living species and supports daily drinking, cultivation, and washing. In the modern era, water resources are being polluted due to effluents from various industries and noxious organic pollutants such as pesticides, cationic/anionic organics, pesticide dyes (methylene blue), and nitro compounds (4-nitrophenol) (Homaeigohar, 2020; Liu, 2020). These pollutants have various applications such as methylene blue (MB); a thiazine dye is being utilized in the textile, data storage, and holographic industries. It is used as an antimalarial and as a chemotherapeutic agent. It is additionally used for staining body tissues during surgeries and diagnosis. These organic pollutants negatively influence human existence by damaging body organs such as the excretory, nervous, and immune systems (Caplin et al., 2019; Manisalidis et al., 2020). By discharging them into the hydrosphere, an environment imbalance is being caused due to the formation of thick, sloppy layer in the aquatic systems. It diminishes the oxygen (O_2) absorbing capacity of water and restricts sunlight penetration which in turn harms the aquatic life. Some valuable groups such as organic dyes produced during the physiochemical process are profoundly responsible. Industrial effluents pollute the water bodies due to the presence of organic dyes and nitro pollutants which

* Corresponding authors at: Department of Chemical Engineering, University Centre for Research and Development, Chandigarh University, Gharuan, Mohali 140413, India.
E-mail addresses: jagpreetnano@gmail.com, jagpreet.e12147@cumail.in (J. Singh), mohitnano.nit@gmail.com (M. Rawat), kumarsanju25@gmail.com (S. Kumar).
Deceased author.

Peer review under responsibility of King Saud University.

Production and hosting by Elsevier

https://doi.org/10.1016/j.jksus.2022.102059
1018-3647/

are highly reactive and tend to form covalent bonds with substrates such as protein molecules and organic fibers. These organic dyes and nitro pollutants have a long half-life and subsequently persist in the environment (Berradi et al., 2019; Lellis et al., 2019). Thus, there exists a need to eliminate these pollutants from water quickly without creating any harmful by-products.

The toxic dyes can be reduced from contaminated water with several physical and chemical routes (Sharma and Bhattacharya, 2017). Some of these processes are more dangerous than the primary pollutants, which are energy-consuming interactions. The utilization of organic solvents has a simple alternate in the form of the shift towards nanoparticles (NPs). Nanoparticles have a large surface relative to volume, generating reactive oxygen species (ROS). Surface plasmon resonance (SPR) helps to increase the efficiency of degradation of pollutant photocatalysis dyes (Panimalar et al., 2020; Renuka et al., 2020; Vinayagam et al., 2022). On the other hand, 4-nitrophenol (4-NP) is a phenolic compound consisting of the nitro group at the position of a hydroxyl group of the benzene ring. There are numerous applications of 4-NP i.e., utilization in drugs, fungicides, dyes, and for darkening the leather (Tchieno and Tonle, 2018). However, when this nitro pollutant is mixed with fresh water, it can exhaust water bodies to a larger extent which causes skin problems, eyes infections, and blood disorders. It also decreases O_2 carrying capacity of the blood to tissues of aquatic species and human beings. This interaction is significant for both natural and mechanical elements due to various reasons.

Although various strategies such as adsorption, reverse osmosis, or chemical coagulations are available for wastewater treatment, they may be insufficient and ineffective for reducing nitro pollutants (Kumar et al., 2012). The conversion of 4-NP into 4-aminophenol (4-AP) is not easy, as it is exceptionally stable and poorly soluble in water. The reduction of 4-NP is a vital subject in current research. During the past decade, the reduction of nitrophenols into amino-phenols using metal nanoparticles (MNPs) has merited consideration. Because of this, the whole reaction is completed in an aqueous solution at room temperature. However, without NPs, the reaction requires more than three days for completion, which is also insufficient. For detoxification and decolorizing of a nitro compound, chemical reduction strategies are utilized with the assistance of MNPs, which can act as reaction catalysts and assist in lowering the kinetic barrier by moving electrons from donor to BH_4. Nanoparticles have a large surface area relative to volume, increasing the interaction between reactant molecules (Ijaz et al., 2020; Jayakumar et al., 2017; Sathiyaraj et al., 2021; Sharma et al., 2019). However, antimicrobial activity is regulated by the capacity of compounds to control or reduce the bacterial growth rate (Kasinathan et al., 2016; Maria Magdalane et al., 2018; Mobeen Amanulla et al., 2018; Subba Reddy et al., 2018). The compound contains mediator molecules, it may either be bactericidal and/or bacteriostatic in nature. Since most of the antimicrobial agents existing in the pharmaceutical market are either chemically synthesized or naturally appearing.

Accordingly, gold nanoparticles (Au NPs) can be applied at various levels i.e., as photocatalyst and antimicrobial agents to decrease several types of organic pollutants like 4-NP and microbial pathogens from aquatic environments, respectively. The Au NPs are synthesized through various approaches like chemical, electrochemical, laser ablation, and synchrotron radiations (Daruich De Souza et al., 2019). Unfortunately, in these processes, noxious and highly reactive chemicals are involved which obstruct their demand in many applications. Subsequently, there is a great need for an eco-friendly, sustainable, and cost-effective approach for synthesizing metal NPs, which fulfill the voids present in chemical processes. Green synthesis of Au NPs can be a good alternative over conventional ones as it involves the production of NPs by utilizing inherent resources just as plants and microorganisms (Rani et al., 2020; Singh et al., 2019b, 2018a). This approach has garnered a lot of attention in the previous decade, especially for silver (Ag) and gold (Au) NPs, which are far more stable than other metal NPs. Green NPs synthesizing technologies are easily scaled up and offer a variety of benefits, including environmental friendliness, economic feasibility, affordability, safety, and speed, as well as organic capping and stability aspects (Singh et al., 2019a, 2018b; Verma et al., 2020). Several studies for the green production of Au NPs through different medicinal plants such as *Acorus calamus, Alternanthera dentate, Ocimum sanctum, Azadirachta indica, Brassica rapa, Coccinia indica, Vitex negundo, Melia dubia,* have been reported (Naikoo et al., 2021).

In this look, the present work validates a novel, green, and sustainable synthesis of Au NPs with leaf extract of *Ananas comosus* wastes. *A. comosus* is a natural fruit classified under the family of Bromeliaceae. The fruit contains bromelain as a phytochemical that assists in reducing and stabilizing the formation of Au NPs. The synthesized Au NPs have been employed as catalyst (nitrophenol reduction), photocatalyst (degradation of methylene blue), and antimicrobial agent (towards *Escherichia coli* and *Bacillus subtilis*). Additionally, Au NPs have been found stable for a significant period, which is a fundamental part of each industrial application. Therefore, the present study indicates the conversion of waste to value added product.

2. Experimental section

2.1. Materials

Firstly, *A. comosus* waste leaves were collected from the garden areas in Punjab (India). Chloroauric corrosive (methylene blue dye, 4-NP, sodium borohydride ($NaBH_4$)), Luria Broth (LB), Agar, Petri plates, sodium hydroxide (NaOH), and hydrochloric acid (HCl) were purchased from Merck, Germany. All the glasswares were cleaned properly before to use with freshly prepared piranha solution (consists of concentrated H_2SO_4/H_2O_2 (3:1)), succeed by distilled water.

2.2. Preparation of aqueous A. comosus leaf extract

10 g of *A. comosus* leaves were splashed with water to remove dust and other contaminants. Air-dried A. comosus leaves were cut into small pieces and added into 100 mL of distilled water (DI). Then, mixture was boiled for 45 min at 80 °C. After appearing greenish-yellow color, the mixture was filtered using Whatman filter paper and obtained extract was stored. Different pH was maintained using NaOH and HCl for alkaline and acidic, respectively.

2.3. Synthesis of Au NPs using aqueous A. comosus leaf extract

100 mL of DI water was boiled at 100 °C for 1 h. The 10^{-3} M chloroauric acid ($HAuCl_4$) was added dropwise to the boiling water. The solution was stirred continuously for 15 min, and 1 mL of leaf extract was added into it dropwise. The solution changed color immediately from greenish-yellow to wine red, which can be regulated for the formation Au NPs.

2.4. Catalytic activity of AuNPs

UV–Vis absorption spectrum was observed for the catalytic reduction reaction of 4-NP. Firstly, 200 μL of 10^{-1} M $NaBH_4$ reaction with 30 μL of 10^{-2} M 4-NP and 2.7 mL of DI water was spectrophotometrically observed at different time intervals. The progressive color change from bright yellow to colorless was detected during the reaction and it confirmed the development of 4-AP. The differ-

ent volume of catalyst (5, 10, and 15 μL) was added and reduction process time interval was recorded.

2.5. Evaluation of antimicrobial activity

For determining the antimicrobial activity of synthesized Au NPs, a well-plate diffusion technique was utilized. Firstly, for microbial cultural growth, Luria broth and agar-agar type 2 solutions were spread on Petri plates and incubated overnight at 37 °C. Then, the bacteria (*Escherichia coli and Bacillus subtilis*) were spread on the Luria broth plate. The plates were punched and Au NPs were added at different volumes (60, 80, 100, 120, 140 μL) and then placed overnight at 37 °C for 24 h.

2.6. Photocatalytic degradation of organic dyes by Au NPs

In the presence of sunlight radiation, 30 ppm MB dye was reduced with the assist of Au NPs. For the recognition of adsorption–desorption equilibrium, the organic dye was first dissolved into DI water. The reduction of dye was also tested without including a photocatalyst underneath sunlight exposure. Then, after the addition of 10 mg of Au NP catalyst, dye solution was stirred and sonicated for 10 min. Finally, the aqueous solution was kept under natural sunlight for 180 min. 5 3 mL of dye solution was taken at regular interval of time and was centrifuged for 15 min at 10,000 rpm for photocatalyst partition. Later, 2 mL of supernatant was recovered and the absorption spectrum was recorded and examined. The maximum absorbance intensity of dye solution was observed at wavelength of 665 nm. The absorbance intensity of dye solution was declined with time due to dye degradation. Therefore, the efficiency of dye degradation (R) was envisioned as follows [Mehta et al., 2016];

$$R = (C_0 - C_t)/C_0 \quad (1)$$

where C_0 and C_t are the concentrations of MB dye solution at time t = 0 and t = 20 min, 40 min, 60 min, 80 min, 100 min, 120 min, respectively.

2.7. Characterization of synthesized Au NPs

Optical investigation of synthesized Au NPs was attempted through UV–Visible spectrophotometer (UV–Vis; UV-2600, Shimadzu) using absorbance versus wavelength spectrum having wavelength range 200 to 800 nm. Fourier transform infrared spectrophotometer (FTIR; Alpha Bruker Corp.) was used to detect the presence of phytochemicals in Ananas waste extract and on the surface of Au NPs. The average size of particles was determined with particle size analyzer (Malvern-ZEN-1690). The specific particles size and the morphological studies were carried out by a high-resolution transmission electron microscope (HRTEM; Jeol JEM-2100). Similarly, the crystalline arrangement and interplanar d-spacing between lattice planes were examined by selected area electron diffraction (SAED).

3. Results

A. comosus leaf extract acts as a reducing, and stabilizing agent whereas $HAuCl_4$ is the gold precursor. The reduction of $HAuCl_4$ was evidenced by the change in leaf extract color during the experiment. The reaction was quick as the greenish-yellow color of *A. comosus* leaf extract changed to a wine-red color within a few minutes, it validates the development of Au NPs. The conceivable equation for the formation of Au NPs was $HAuCl_4$ (aq) + *A. comosus* leaf extract = Au NPs (See Fig. 1).

3.1. UV–Visible spectra

Fig. 2(a & b) show the UV–Vis spectra of *A. comosus* leaf extract and *A. comosus* leaf extract mediated Au NPs, respectively. Fig. 2(b) displays the surface plasmon resonance around wavelength of 520 nm for Au NPs. Fig. 2(c) shows the UV–Vis spectra of Au NPs at different pH values. It was observed that at the acidic medium (pH < 7), a redshift with a broad absorption band was observed which indicated the increase in size and broad particle size distribution, inadequate accessibility of stabilizing (OH– functional groups) (Bogireddy et al., 2018). In contrast, at alkaline medium (pH > 7), a sharp absorption band with blue shift was observed which ascribed the narrow particle size distribution (Bogireddy et al., 2018; Yang et al., 2019). Furthermore, for stability study, UV–Vis spectra of Au NPs after one year was recorded as shown in Fig. 2d. A slight change in absorbance value confirmed the remarkable consistency of Au NPs.

3.2. Fourier transform infrared spectroscopy (FTIR) analysis

Fig. 3 shows the FTIR spectra obtained from pure *A. comosus* leaf extract and synthesized Au NPs. In Au NPs spectrum, the band at 3751 cm^{-1} is due to stretching of –OH bond which clarifies the existence of benzophenones, anthocyanins phenol and flavonoid groups present in the Ananas leaf extract. The band at 1696 cm^{-1} and 1380 cm^{-1} are attributed towards the C-O stretching of amide-I and C-N stretching of amine, respectively (Kureshi et al., 2021). Region of 2903–2944 cm^{-1} corresponds to the presence of C–H bond stretching. Bands around 1062 cm^{-1} are due to C=O bond stretching in the ethers, alcohols and polyphenols which are present in leaf extract. Thus, the FTIR analysis indicates that the reduction of Au^{3+} to Au^0 and stabilization are carried out by the involvement of phenolic compounds (Boruah et al., 2021; Botteon et al., 2021).

3.3. High resolution transmission electron microscope (HRTEM) micrographs

Fig. 4 (a) displays typical HR-TEM micrographs of Au NPs having morphology of different defined shapes. Spherical, triangular, pyramidal and other different shapes have been observed as shown in Fig. 4(a). The bar scale in HRTEM micrograph depicts the dimensions of particles are in nanometer range. It has been found that the particle size range is 20 nm to 30 nm. HRTEM micrograph depicts the lattice spacing of 0.21 nm and it elucidates the growth of the Au NPs is mostly in the (111) plane. Fig. 4 (d) displays the SAED pattern consisting concentric bright rings and sharp diffraction spots attributing due to lattice-reflections from different diffraction planes of Au NPs which clearly indicate the crystalline nature of synthesized particles. SAED findings also show that the *fcc* structure of Au NPs conforming to the (111), (200), (210), and (311) crystalline planes.

3.4. Catalytic reduction studies

The catalytic effectiveness of synthesized Au NPs was scrutinized and showed complete decline for the amount of 4-NP in the presence of $NaBH_4$ reductant. At first, in the incidence of $NaBH_4$.

(t = 0), the UV–Vis spectrum (Fig. 5) shows the band at wavelength of 400 nm due to development of Nitrophenolate ion. Subsequently, due to accumulation of Au NPs in the solution, the absorption intensity is decreased at 400 nm with simultaneous decrease in comparatively broader band at 298 nm of amino phenol ions. The catalytic capacity of synthesized Au NPs is evaluated by using diverse volumes i.e., 5 μL, 10 μL, and 15 μL (Fig. 5 (a, b &

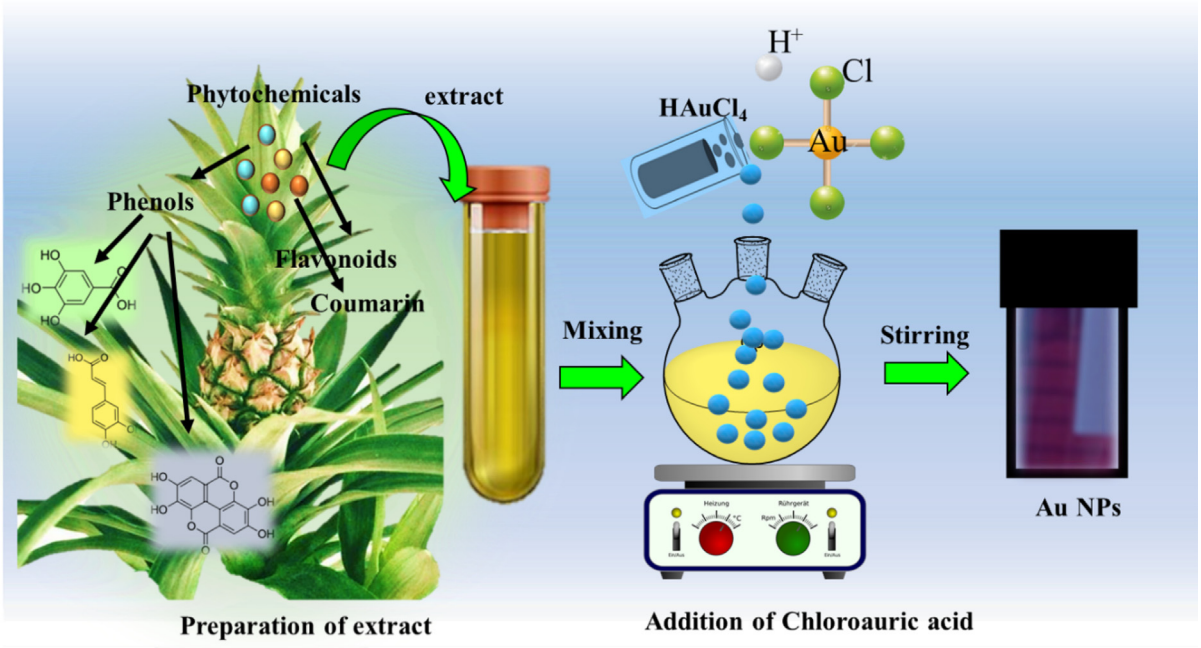

Fig. 1. Schematic representation of *A. comosus* leaf extract mediated Au NPs.

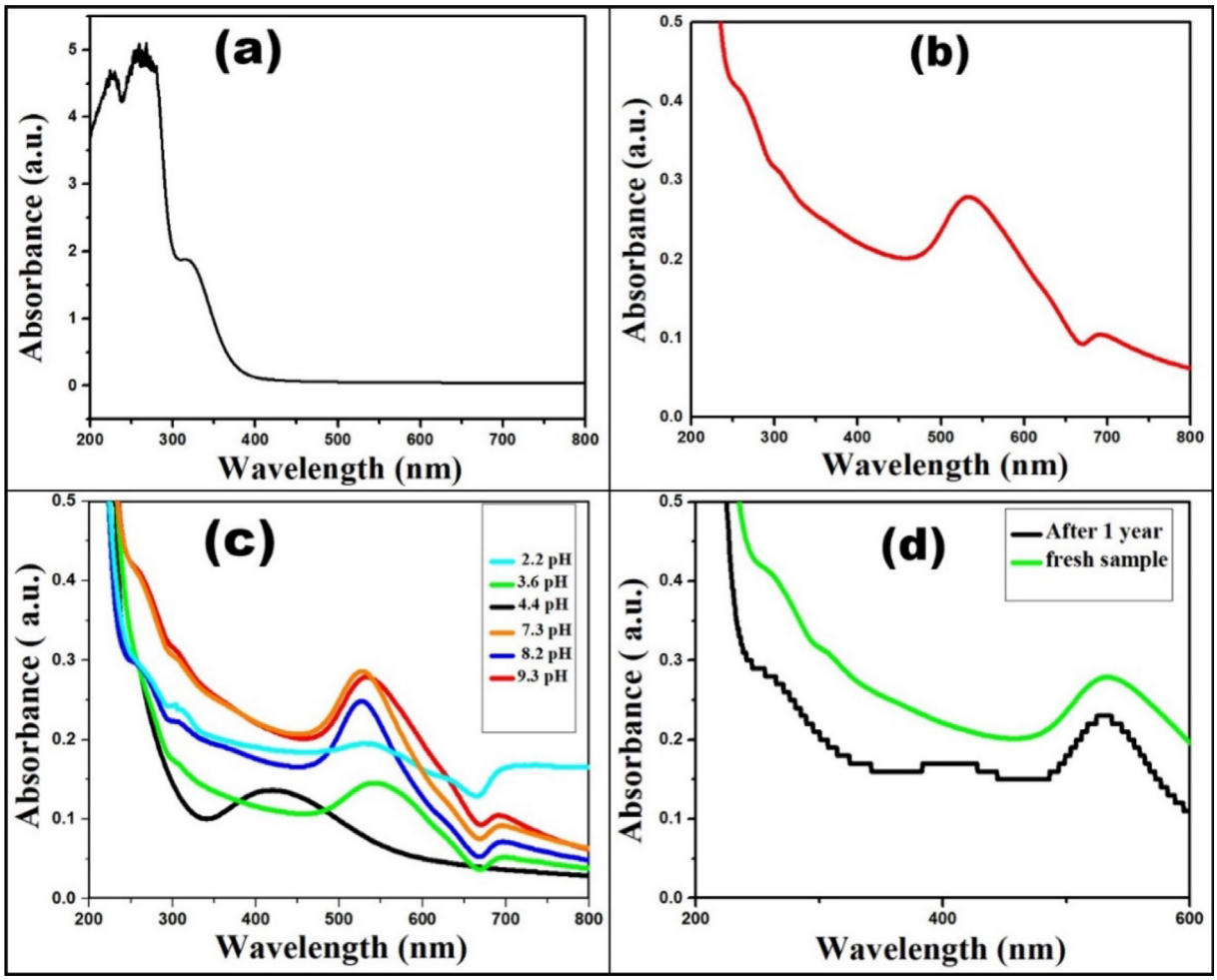

Fig. 2. (a & b) UV–Vis spectra of leaf extract and synthesized Au NPs, (c) effect of pH on Au NPs, and (d) stability study of Au NPs after one year.

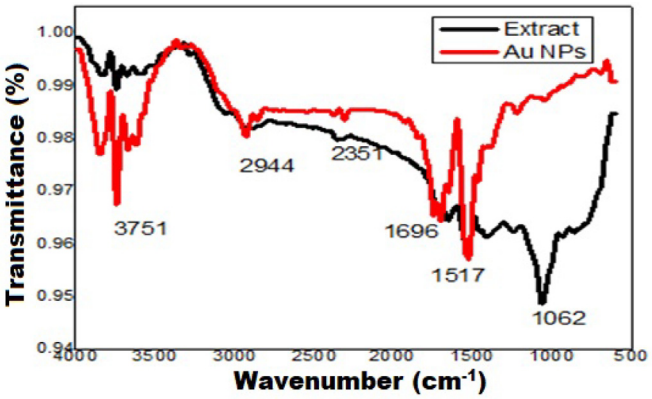

Fig. 3. FTIR spectra of Au NPs and *Ananas comosus* leaf extract.

c). It has been clearly seen that using 5 µL and 10 µL volume of Au NPs, time taken for the complete reduction of 4-NP is 70 min and 60 min, respectively. While, 15 µL of Au NPs is the optimum amount at which complete 4-NP reduction is observed within 20 min (Fig. 5(c)). The kinetic plot i.e., $\ln(C_t/C_0)$ versus time, depicts that it is pseudo-first-order kinetic reaction. The apparent rate constant (K_{appa}) value is found to be 0.1552 min^{-1} with a regression coefficient (R^2) of 0.949. Here, R^2 value (>0.9) confirms the fact that experimental data fits well and catalytic reaction trails pseudo-first-order kinetics (Alhaji et al., 2019; Mangala Nagasundari et al., 2021; Subbareddy et al., 2020).

3.5. Antimicrobial activity of AuNPs

Antimicrobial property of synthesized AuNPs was assessed towards Gram positive and negative bacteria such as *B. subtilis* and *E. coli*, respectively. Different concentrations of solution of synthesized Au NPs were introduced into *E. coli* and *B. subtilis* culture petri plates using disk-diffusion methods, as displayed in Fig. 6. Four wells of the petri plate were occupied with 60, 80, 100, 120, and 140 µL suspension of Au NPs (Fig. 6). Different inhibition zone was exhibited in all AuNPs-treated wells, whereas no inhibition zone was noticed in control petri plates (Table 1). The inhibition zone exposed directly proportional to the concentration of Au NPs (Mani et al., 2021a, 2021b).

3.6. Photocatalytic activity of Au NPs for the degradation of MB dye

To determine the degradation potency, the experiment was performed with and without catalyst in the dark and then in the presence of sunlight. The photocatalytic activity of Au NPs towards the degradation of an organic dye (MB dye) has been evaluated using UV–Vis spectrophotometer. Fig. 7 shows that an absorption peak for the aqueous solution of MB dye is observed at a wavelength of 665 nm. After the addition of Au NPs (50 µL) into the dye solution and then placing it under the exposure of daylight, it has been observed that the absorption peak has started to decline at regular interval of time, as displayed in Fig. 7(a). Also, during the experiment, it has been found that the color of dye solution fades away with the time as the peak intensity decreases. Finally, when the color of solution becomes almost colorless, the peak intensity has

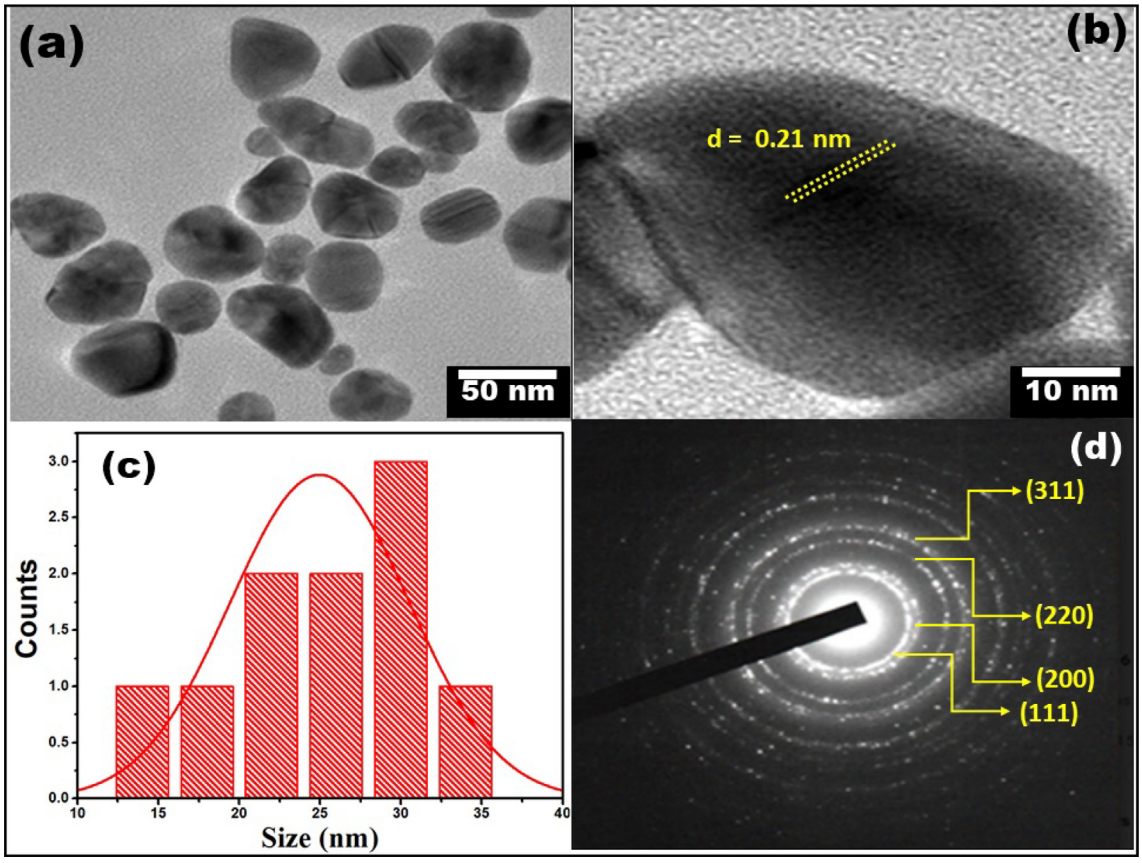

Fig. 4. (a-b) HRTEM micrograph, (c) particle size distribution curve, and (d) SEAD pattern of synthesized Au NPs.

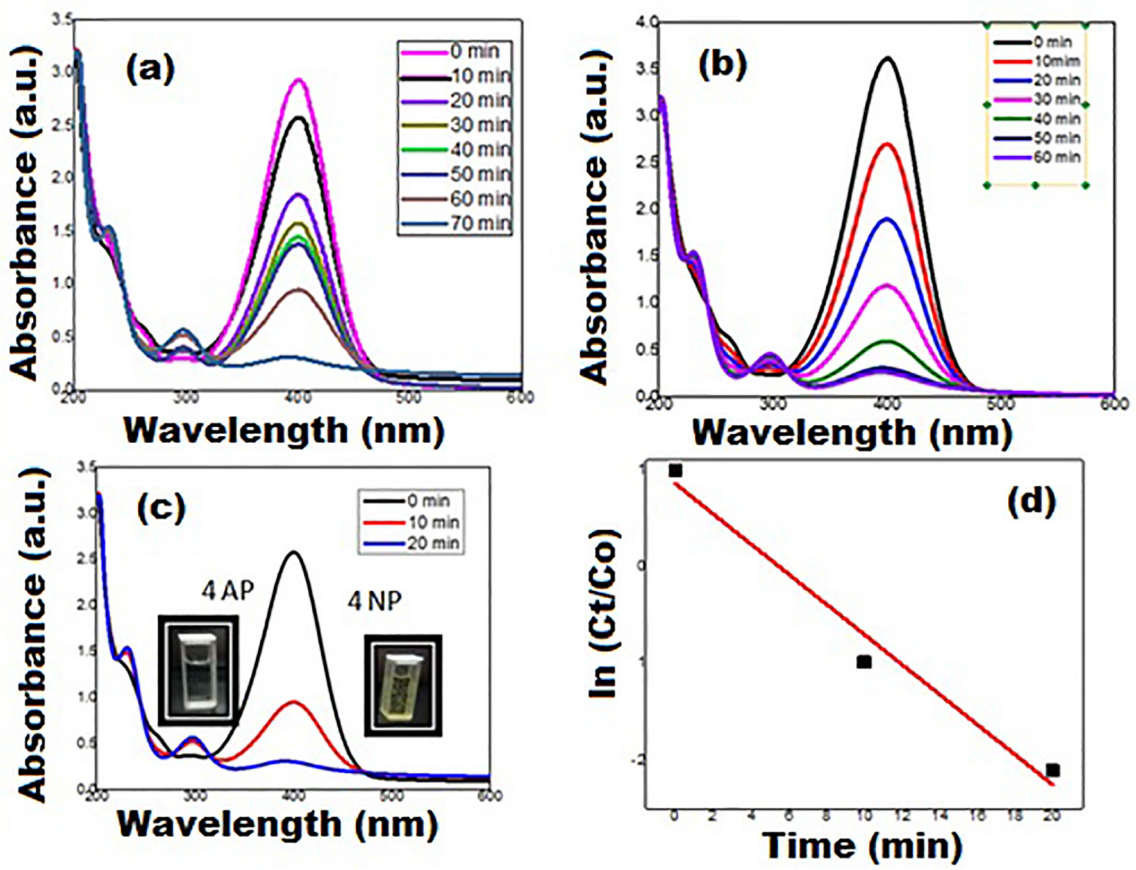

Fig. 5. (a, b & c) UV–Vis spectra of 4-NP reduction using different volume of Au NPs i.e., 5 µL, 10 µL, and 15 µL, respectively, and (d) Kinetic study for the reduction of 4-NP.

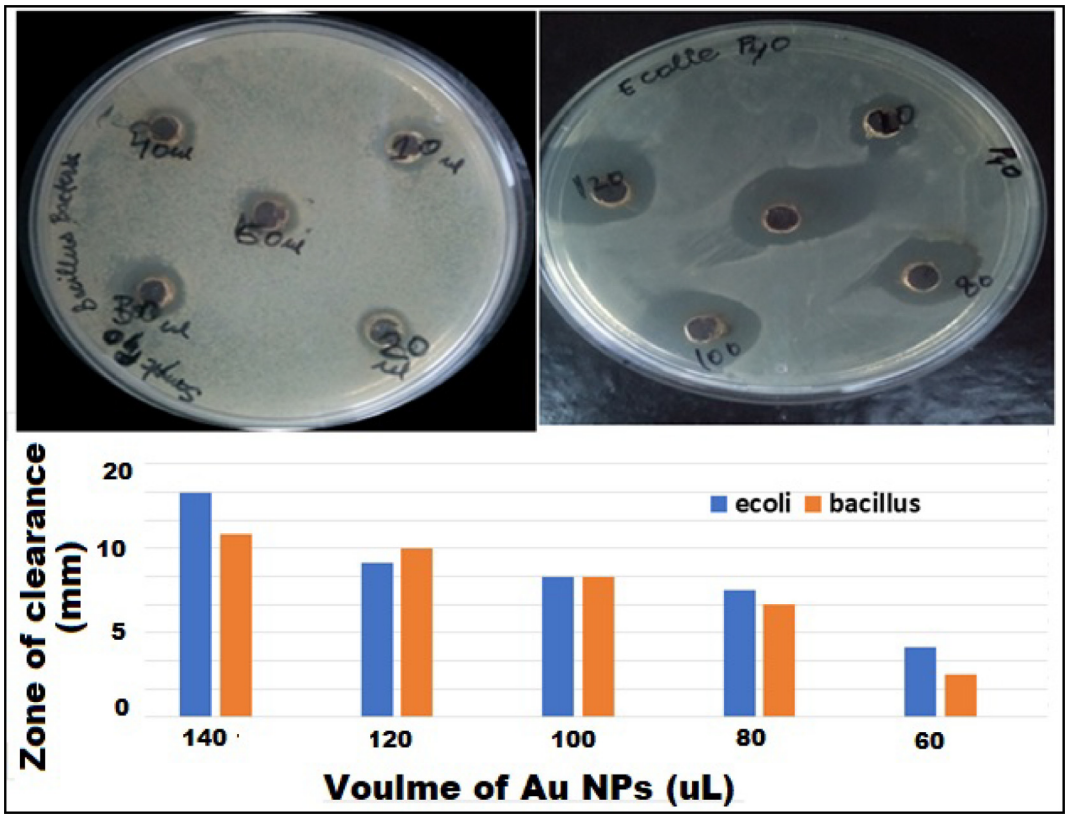

Fig. 6. Antimicrobial activity against *Escherichia coli and Bacillus subtilis* and a histogram (zone of clearance versus volume of catalyst).

also approached the base line and complete MB dye is found to be removed within 130 mins of sunlight exposure. While, the same removal of MB dye at different volumes of Au NPs i.e., 100 μL, 150 μL and 200 μL, is found to be within 110 mins, 100 mins and 80 mins of sunlight exposure, respectively (Fig. 7(b, c and d)). From the kinetic plot i.e., ln (C_t/C_0) vs. time for the degradation of MB dye solution using Au NPs (50 μL, 100 μL, 150 μL and 200 μL), rate constant (K_{appa}) values have been calculated which are mentioned in Fig. 7(e, f, g, and h), respectively. The higher K_{appa} values (~0.04) are observed when 150 μL and 200 μL volume of Au NPs is used in the degradation experiment as compared 50 μL and 100 μL volume of Au NPs. It indicates that the degradation of MB dye is faster at higher volumes of Au NPs. The calculated regression coefficient (R^2) values are also mentioned in Fig. 7(e, f, g, & h) which indicates that the photodegradation experimental data fits well with the pseudo-first- order kinetic model. It has been indicated that plant-mediated NPs have an excellent catalytic potential. The reason for this is that biogenic NPs have a larger specific surface area and more surface active sites (attributed to the prevalence of phytochemicals on the NPs' surface), which promotes adsorption and photocatalytic potency.

4. Discussion

According to mechanistic viewpoint, due to the existence of great activation energy barrier for the reduction of 4-NP into 4-AP, is relatively troublesome free of catalyst. The kinetic barrier rises because of variation among the conversion potential of $BH4^-$ donor and 4-NP acceptor molecule (Rani et al., 2020). Nevertheless, owing the large number of active high surface sites, Au NPs act as electron intermediates and facilitates an electron transmit upshot from donor to acceptor molecules. Consequently, Au NPs competently ease the initiation energy barrier among reactant and product which is favorable for the reduction of 4-NP into 4-AP (Fig. 8).

From the results, it is observed that the synthesized Au NPs exhibited maximum antimicrobial activity against Gram negative bacteria as compared Gram positive bacteria. Since, this different antimicrobial activities were discussed in several earlier reports (Rani et al., 2020). First, there are two different bacteria based on cell wall types, which show some difference. Gram positive bacteria holds thick cell wall and it contains rich peptidoglycan and reduces resistance to Au NPs comparative with Gram negative pathogens with a thin cell wall. Second possible mechanisms may be Gram positive bacteria has a negative charge on them and they can pull Au ions towards the surface and may be the less volume reaches the plasma membrane. Possible antimicrobial mechanisms such as oxidative pressure, DNA destruction, protein denaturation, and cell membrane rupture of Au NPs are described in Fig. 9. Synthesized Au NPs present an efficient antimicrobial effect because of the existence of biomolecules related with commercial and chemically produced NPs. It is recommended that owing small size and huge intake of Au NPs, the Au NPs demonstrate enhanced toxicity towards the microbial pathogens. The formation of ROS species in Au NPs is the main reason for killing the bacterial cell (See Fig. 9).

Table 1
Zone of clearance *w.r.t* different volume of Au NPs.

Sr. No.	Catalyst Volume (μl)	*E. coli* (mm)	*Bacillus* (mm)
1.	140	16	13
2.	120	11	12
3.	100	10	10
4.	80	9	8
5.	60	5	3

5. Conclusions

This present work establishes an inspired and green methodology for the biosynthesis of Au NPs with *A. comosus* leaf extract. Spectroscopic and electron microscopic analysis confirms that synthesized Au NPs are almost of uniform size and distributed at pH of 6. SAED array elucidates that Au NPs are of polycrystalline nature with *fcc* framework. The investigation of catalytic activity of biosynthesized Au NPs is the successful conversion of 4-NP to 4-AP. The reaction kinetics explicating the linear plot indicate towards the pseudo-first-order reaction. The calculated K_{appa} value is found to be 0.1552 min^{-1} at 15 μL of Au NPs. Second approach i.e., photocatalytic reduction of MB dye is accomplished with aid of Au NPs in light-independent and dependent levels. And, almost complete dye has been removed under the exposure of natural sunlight.

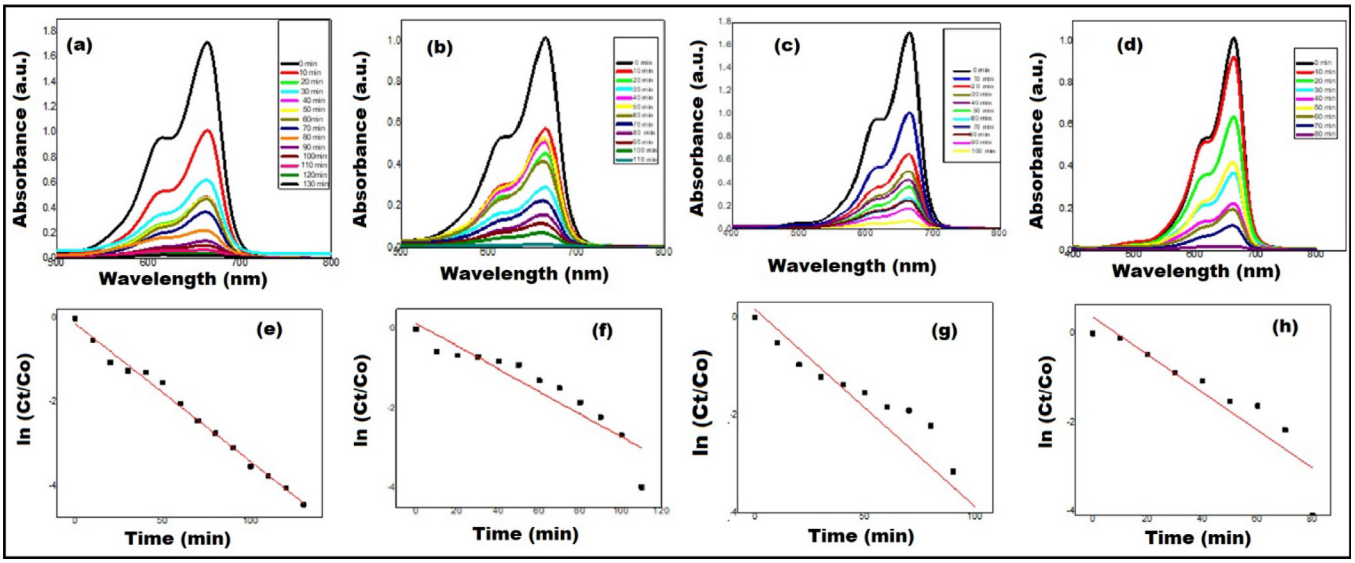

Fig. 7. (a, b, c & d) Photocatalytic activity of Au NPs and (e, f, g & h) Kinetic plots of degradation of MB dye at different volumes of Au NPs (50 μL, 100 μL, 150 μL & 200 μL), respectively.

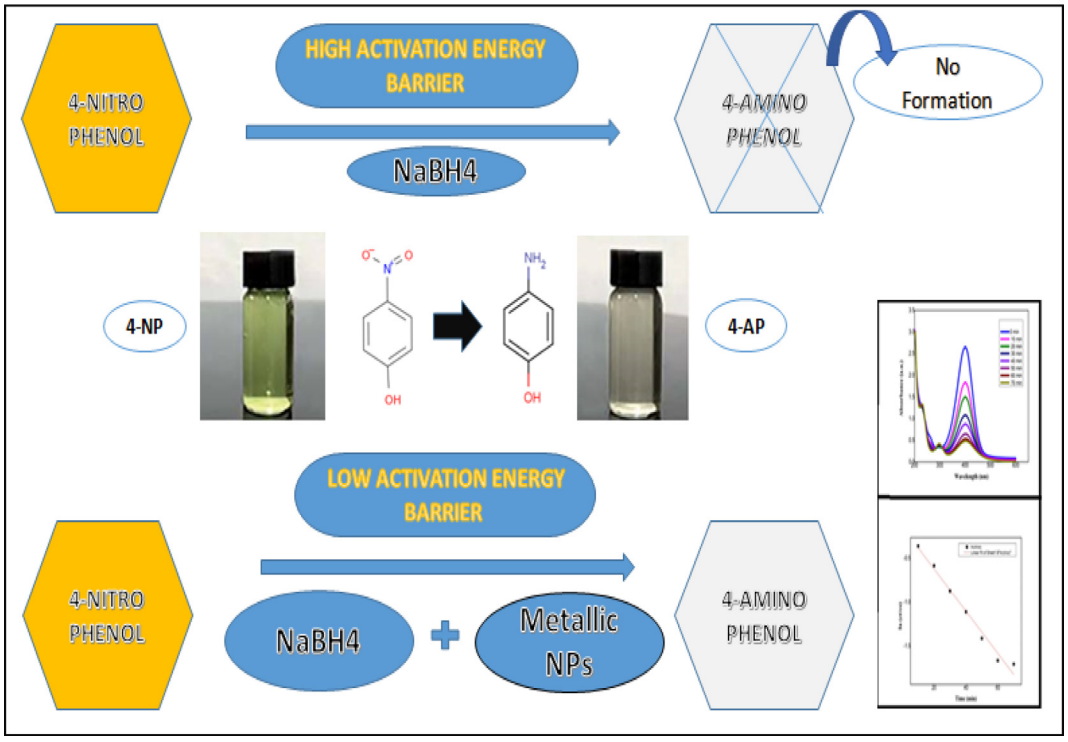

Fig. 8. Schematic representation of the mechanism of catalytic activity of Au NPs.

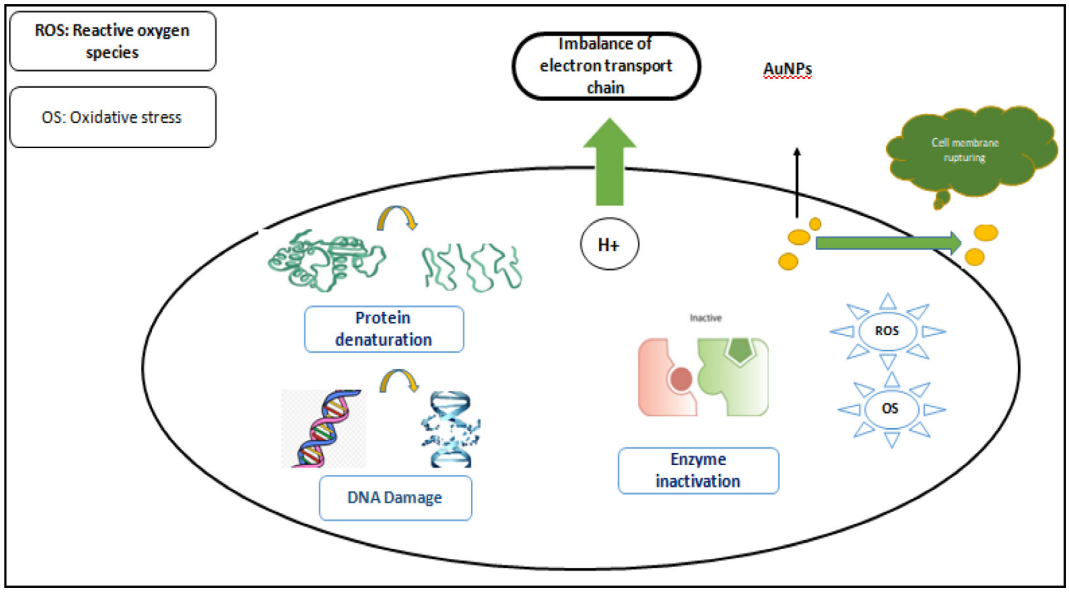

Fig. 9. Mechanism of Antimicrobial activity.

Lastly, the antimicrobial efficiency of Au NPs against *E. coli* and *B. subtilis* is directly increased with the increase in the concentration of Au NPs. Thus, the present study offers a green and cost-effective method for the preparation of Au NPs towards the biomedical and environmental applications.

Declaration of Competing Interest

The authors declare that they have no known competing financial interests or personal relationships that could have appeared to influence the work reported in this paper.

Acknowledgements

The authors gratefully acknowledge Chandigarh University (Mohali, Punjab, INDIA), Sri Guru Granth Sahib World University (Fatehgarh Sahib, Punjab, INDIA) for research lab facilities. JS would like to dedicate this work to the late Prof. Mohit Rawat (Former Head Department of Nanotechnology, Sri Guru Granth Sahib World University), under whose supervision this work was carried out. Authors are thankful to Department of Biotechnology, Sri Guru Granth Sahib World University (Fatehgarh Sahib) and Sprint Testing Solutions (Mumbai) for providing the necessary facilities for

this research work. This project was supported by Researchers Supporting Project number (RSP-2021/230) King Saud University, Riyadh, Saudi Arabia.

References

Alhaji, N.M.I., Nathiya, D., Kaviyarasu, K., Meshram, M., Ayeshamariam, A., 2019. A comparative study of structural and photocatalytic mechanism of AgGaO2 nanocomposites for equilibrium and kinetics evaluation of adsorption parameters. Surf. Interfaces 17, 100375. https://doi.org/10.1016/j.surfin.2019.100375.

Berradi, M., Hsissou, R., Khudhair, M., Assouag, M., Cherkaoui, O., El Bachiri, A., El Harfi, A., 2019. Textile finishing dyes and their impact on aquatic environs. Heliyon 5 (11). https://doi.org/10.1016/j.heliyon.2019.e02711.

Bogireddy, N.K.R., Pal, U., Gomez, L.M., Agarwal, V., 2018. Size controlled green synthesis of gold nanoparticles using Coffea arabica seed extract and their catalytic performance in 4-nitrophenol reduction. RSC Adv. 8, 24819–24826. https://doi.org/10.1039/c8ra04332a.

Boruah, J.S., Devi, C., Hazarika, U., Bhaskar Reddy, P.V., Chowdhury, D., Barthakur, M., Kalita, P., 2021. Green synthesis of gold nanoparticles using an antiepileptic plant extract: in vitro biological and photo-catalytic activities. RSC Adv. 11, 28029–28041. https://doi.org/10.1039/D1RA02669K.

Botteon, C.E.A., Silva, L.B., Ccana-Ccapatinta, G.V., Silva, T.S., Ambrosio, S.R., Veneziani, R.C.S., Bastos, J.K., Marcato, P.D., 2021. Biosynthesis and characterization of gold nanoparticles using Brazilian red propolis and evaluation of its antimicrobial and anticancer activities. Sci. Rep. 11. https://doi.org/10.1038/s41598-021-81281-w.

Caplin, A., Ghandehari, M., Lim, C., Glimcher, P., Thurston, G., 2019. Advancing environmental exposure assessment science to benefit society. Nat. Commun. 10 (1). https://doi.org/10.1038/s41467-019-09155-4.

Daruich De Souza, C., Ribeiro Nogueira, B., Rostelato, M.E.C.M., 2019. Review of the methodologies used in the synthesis gold nanoparticles by chemical reduction. J. Alloy. Compd. 798, 714–740. https://doi.org/10.1016/j.jallcom.2019.05.153.

Homaeigohar, S., 2020. The nanosized dye adsorbents for water treatment. Nanomaterials 10 (2), 295. https://doi.org/10.3390/nano10020295.

Ijaz, I., Gilani, E., Nazir, A., Bukhari, A., 2020. Detail review on chemical, physical and green synthesis, classification, characterizations and applications of nanoparticles. Green Chem. Lett. Rev. 13 (3), 223–245. https://doi.org/10.1080/17518253.2020.1802517.

Jayakumar, C., Magdalane, C.M., Kaviyarasu, K., Kulandainathan, M.A., Jeyaraj, B., Maaza, M., 2017. Direct electrodeposition of gold nanoparticles on glassy carbon electrode for selective determination catechol in the presence of hydroquinone. J. Nanosci. Nanotechnol. 18, 4544–4550. https://doi.org/10.1166/jnn.2018.15307.

Kasinathan, K., Kennedy, J., Elayaperumal, M., Henini, M., Malik, M., 2016. Photodegradation of organic pollutants RhB dye using UV simulated sunlight on ceria based TiO2 nanomaterials for antibacterial applications. Sci. Rep. 6. https://doi.org/10.1038/srep38064.

Kumar, P., Agnihotri, R., Wasewar, K.L., Uslu, H., Yoo, C.K., 2012. Status of adsorptive removal of dye from textile industry effluent. Desalin. Water Treat. 50, 226–244. https://doi.org/10.1080/19443994.2012.719472.

Kureshi, A.A., Vaghela, H.M., Kumar, S., Singh, R., Kumari, P., 2021. Green synthesis of gold nanoparticles mediated by Garcinia fruits and their biological applications. Pharm. Sci. 27, 238–250. https://doi.org/10.34172/PS.2020.90.

Lellis, B., Fávaro-Polonio, C.Z., Pamphile, J.A., Polonio, J.C., 2019. Effects of textile dyes on health and the environment and bioremediation potential of living organisms. Biotechnol. Res. Innov. 3, 275–290. https://doi.org/10.1016/j.biori.2019.09.001.

Liu, Q., 2020. Pollution and treatment of dye waste-water. IOP Conf. Ser.: Earth Environ. Sci. 514 (5). https://doi.org/10.1088/1755-1315/514/5/052001.

Mangala Nagasundari, S., Muthu, K., Kaviyarasu, K., Farraj, D.A.A., Alkufeidy, R.M., 2021. Current trends of Silver doped Zinc oxide nanowires photocatalytic degradation for energy and environmental application. Surf. Interfaces 23. https://doi.org/10.1016/j.surfin.2021.100931.

Mani, M., Harikrishnan, R., Purushothaman, P., Pavithra, S., Rajkumar, P., Kumaresan, S., Al Farraj, D.A., Elshikh, M.S., Balasubramanian, B., Kaviyarasu, K., 2021a. Systematic green synthesis of silver oxide nanoparticles for antimicrobial activity. Environ. Res. 202. https://doi.org/10.1016/j.envres.2021.111627.

Mani, M., Pavithra, S., Mohanraj, K., Kumaresan, S., Alotaibi, S.S., Eraqi, M.M., Gandhi, A.D., Babujanarthanam, R., Maaza, M., Kaviyarasu, K., 2021b. Studies on the spectrometric analysis of metallic silver nanoparticles (Ag NPs) using Basella alba leaf for the antibacterial activities. Environ. Res. 199. https://doi.org/10.1016/j.envres.2021.111274.

Manisalidis, I., Stavropoulou, E., Stavropoulos, A., Bezirtzoglou, E., 2020. Environmental and health impacts of air pollution: A review. Front. Public Heal. https://doi.org/10.3389/fpubh.2020.00014.

Maria Magdalane, C., Kaviyarasu, K., Matinise, N., Mayedwa, N., Mongwaketsi, N., Letsholathebe, D., Mola, G.T., AbdullahAl-Dhabi, N., Arasu, M.V., Henini, M., Kennedy, J., Maaza, M., Jeyaraj, B., 2018. Evaluation on La2O3 garlanded ceria heterostructured binary metal oxide nanoplates for UV/visible light induced removal of organic dye from urban wastewater. South Afr. J. Chem. Eng. 26, 49–60. https://doi.org/10.1016/j.sajce.2018.09.003.

Mobeen Amanulla, A., Jasmine Shahina, S.K., Sundaram, R., Maria Magdalane, C., Kaviyarasu, K., Letsholathebe, D., Mohamed, S.B., Kennedy, J., Maaza, M., 2018. Antibacterial, magnetic, optical and humidity sensor studies of β-CoMoO4 - Co3O4 nanocomposites and its synthesis and characterization. J. Photochem. Photobiol. B Biol. 183, 233–241. https://doi.org/10.1016/j.jphotobiol.2018.04.034.

Naikoo, G.A., Mustaqeem, M., Hassan, I.U., Awan, T., Arshad, F., Salim, H., Qurashi, A., 2021. Bioinspired and green synthesis of nanoparticles from plant extracts with antiviral and antimicrobial properties: A critical review. J. Saudi Chem. Soc. 25 (9). https://doi.org/10.1016/j.jscs.2021.101304.

Panimalar, S., Uthrakumar, R., Selvi, E.T., Gomathy, P., Inmozhi, C., Kaviyarasu, K., Kennedy, J., 2020. Studies of MnO2/g-C3N4 hetrostructure efficient of visible light photocatalyst for pollutants degradation by sol-gel technique. Surf. Interfaces 20. https://doi.org/10.1016/j.surfin.2020.100512.

Rani, P., Kumar, V., Singh, P.P., Matharu, A.S., Zhang, W., Kim, K.-H., Singh, J., Rawat, M., 2020. Highly stable AgNPs prepared via a novel green approach for catalytic and photocatalytic removal of biological and non-biological pollutants. Environ. Int. 143. https://doi.org/10.1016/j.envint.2020.105924.

Renuka, R., Devi, K.R., Sivakami, M., Thilagavathi, T., Uthrakumar, R., Kaviyarasu, K., 2020. Biosynthesis of silver nanoparticles using phyllanthus emblica fruit extract for antimicrobial application. Biocatal. Agric. Biotechnol. 24, 101567. https://doi.org/10.1016/j.bcab.2020.101567.

Sathiyaraj, S., Suriyakala, G., Dhanesh Gandhi, A., Babujanarthanam, R., Almaary, K. S., Chen, T.W., Kaviyarasu, K., 2021. Biosynthesis, characterization, and antibacterial activity of gold nanoparticles. J. Infect. Public Health 14, 1842–1847. https://doi.org/10.1016/j.jiph.2021.10.007.

Sharma, D., Kanchi, S., Bisetty, K., 2019. Biogenic synthesis of nanoparticles: A review. Arab. J. Chem. 12 (8), 3576–3600.

Sharma, S., Bhattacharya, A., 2017. Drinking water contamination and treatment techniques. Appl. Water Sci. 7, 1043–1067. https://doi.org/10.1007/s13201-016-0455-7.

Singh, J., Dutta, T., Kim, K.-H., Rawat, M., Samddar, P., Kumar, P., 2018a. "Green" synthesis of metals and their oxide nanoparticles: Applications for environmental remediation. J. Nanobiotechnology. 16 (1). https://doi.org/10.1186/s12951-018-0408-4.

Singh, J., Kumar, V., Kim, K.-H., Rawat, M., 2019a. Biogenic synthesis of copper oxide nanoparticles using plant extract and its prodigious potential for photocatalytic degradation of dyes. Environ. Res. 177. https://doi.org/10.1016/j.envres.2019.108569.

Singh, J., Kumar, V., Singh Jolly, S., Kim, K.H., Rawat, M., Kukkar, D., Tsang, Y.F., 2019b. Biogenic synthesis of silver nanoparticles and its photocatalytic applications for removal of organic pollutants in water. J. Ind. Eng. Chem. 80, 247–257. https://doi.org/10.1016/j.jiec.2019.08.002.

Singh, J., Mehta, A., Rawat, M., Basu, S., 2018b. Green synthesis of silver nanoparticles using sun dried tulsi leaves and its catalytic application for 4-Nitrophenol reduction. J. Environ. Chem. Eng. 6, 1468–1474. https://doi.org/10.1016/j.jece.2018.01.054.

Subba Reddy, Y., Maria Magdalane, C., Kaviyarasu, K., Mola, G.T., Kennedy, J., Maaza, M., 2018. Equilibrium and kinetic studies of the adsorption of acid blue 9 and Safranin O from aqueous solutions by MgO decked FLG coated Fuller's earth. J. Phys. Chem. Solids 123, 43–51. https://doi.org/10.1016/j.jpcs.2018.07.009.

Subbareddy, Y., Kumar, R.N., Sudhakar, B.K., Reddy, K.R., Martha, S.K., Kaviyarasu, K., 2020. A facile approach of adsorption of acid blue 9 on aluminium silicate-coated Fuller's Earth––Equilibrium and kinetics studies. Surf. Interfaces 19. https://doi.org/10.1016/j.surfin.2020.100503.

Tchieno, F.M.M., Tonle, I.K., 2018. P-Nitrophenol determination and remediation: An overview. Rev. Anal. Chem. 37. https://doi.org/10.1515/revac-2017-0019.

Verma, V., Singh, M., Pal Singh, P., Singh, J., Rawat, M., 2020. Highly stable Au/Ag core-shell nanoparticles prepared via novel green approach for the abatement of nitro pollutants. Micro Nano Lett 15 (12), 822–825. https://doi.org/10.1049/mnl.2020.0275.

Vinayagam, R., Patnaik, Y., Brijesh, P., Prabhu, D., Quadras, M., Pai, S., Narasimhan, M.K., Kaviyarasu, K., Varadavenkatesan, T., Selvaraj, R., 2022. Superparamagnetic hematite spheroids synthesis, characterization, and catalytic activity. Chemosphere 294,. https://doi.org/10.1016/J.CHEMOSPHERE.2022.133730 133730.

Yang, B., Qi, F., Tan, J., Yu, T., Qu, C., 2019. Study of green synthesis of ultrasmall gold nanoparticles using citrus sinensis peel. Appl. Sci. 9 (12), 2423.